Quantum criticality out of equilibrium in the pseudogap Kondo model

Chung-Hou Chung and Kenneth Yi-Jie Zhang
Electrophysics Department, National Chiao-Tung University, HsinChu, Taiwan 300, Republic of China
(Received 7 August 2011; revised manuscript received 19 April 2012; published 3 May 2012)

Quantum phase transitions out of equilibrium are outstanding emergent subjects in condensed matter physics with great fundamental importance and challenges. We theoretically investigate here the nonequilibrium quantum phase transition in a generic nano-setup: the pseudogap Kondo model where a Kondo quantum dot couples to two—left (L) and right (R)—voltage-biased fermionic leads with power-law density of states (DOS) with respect to their Fermi levels $\mu_{L/R}$, $\rho_{c,L(R)}(\omega) \propto |\omega - \mu_{L(R)}|^r$ with $0 < r < 1$. In equilibrium ($\mu_L - \mu_R = 0$) and for $0 < r < 1/2$, with increasing Kondo correlations this model exhibits a quantum phase transition from a unscreened local moment (LM) phase to the Kondo screened phase. At finite bias voltages and near criticality, we discover new nonequilibrium universal scaling behaviors in conductance, conduction electron T matrix, and local spin susceptibility via a controlled frequency-dependent renormalization group (RG) approach. The current-induced decoherence is key to understanding these distinct universal nonequilibrium quantum critical regimes. The relevance of our results to experiment is discussed.

DOI: 10.1103/PhysRevB.85.195106 PACS number(s): 73.43.Nq, 72.15.Qm, 73.21.La, 73.23.−b

I. INTRODUCTION

Quantum phase transitions (QPTs),[1] the continuous phase transitions that occur at zero temperature due to quantum fluctuations, in strongly correlated electron systems have attracted much attention over the last three decades. Near the quantum critical points (QCPs) associated with QPTs, thermodynamic properties exhibit non-Fermi liquid properties and universal scalings. Recently, due to high tunability, nano-devices such as quantum dots in the Kondo regime[2,3] offer an opportunity to study new aspects in QPTs under nonequilibrium conditions, which has become one of the outstanding emergent subjects in condensed matter physics, with great fundamental importance. Examples include the distinct nonlinear steady-state conductance compared to its equilibrium counterpart in a two-dimensional superconductor-insulator transition,[4] in itinerant magnetism,[5] and in Kondo quantum dots coupled to dissipative environments (e.g., spin[6–8] and charge[9] fluctuations as well as electron-electron interactions in the leads[10]). Outstanding issues include the following: Do universal nonequilibrium scaling functions near QCPs exist? If so, how are they different from their equilibrium counterparts and how can they be realized experimentally? In Ref. 9, the authors discovered the distinct nonequilibrium profile in transport near the localized-delocalized QPT of the Kosterlitz-Thouless (KT) type in a generic voltage-biased dissipative resonance level (quantum dot) from its equilibrium properties at finite temperatures. The current-induced decoherence rate smearing out the transition shows highly nonlinear voltage dependence, resulting in these distinct behaviors.

In this paper, we theoretically address the above issues by investigating the nonequilibrium quantum criticality in a different class of generic nano-setup: the pseudogap Kondo (PGK) model[11–15] in a quantum dot.[16] We consider a Kondo quantum dot coupled to two—left (L) and right (R)—fermionic leads with a power-law (pseudogap) density of states (DOS) which vanishes at the Fermi level $\mu_{L(R)} = \pm V/2$, $\rho_{c,L(R)}(\omega) \propto |\omega - \mu_{L(R)}|^r$ with $0 < r < 1$. Possible realizations of the pseudogap leads include d-wave superconductors ($r = 1$),[14] graphene[17] ($r = 1$), one-dimensional Luttinger systems ($r > 0$),[12] quantum dots embedded in an Aharonov-Bohm ring ($r = 2$),[18] and Kondo quantum dots coupled to magnetic metal leads ($0 < r < 1$).[6–8] In equilibrium ($V = 0$) and for $0 < r < 1/2$, with decreasing Kondo couplings the particle-hole (p-h) symmetric PGK model exhibits a "true" QPT (distinct from a QPT of the KT type[19]) from the Kondo screened phase to the unscreened local moment (LM) phase.[12,14] Near QCP separating these two phases, all observables in equilibrium exhibit universal power-law scalings and have been extensively studied.[14,15] Nevertheless, there is lack of understanding regarding their corresponding out-of-equilibrium quantum critical properties. We shall address below this issue and focus on universal nonequilibrium scaling behavior near the QCP.

II. THE MODEL AND THE RG APPROACH

The Hamiltonian of the particle-hole (p-h) symmetric PGK model reads

$$H = \sum_{k\alpha} (\epsilon_{k\alpha} - \mu_\alpha) c_k^\dagger c_k + \sum_{\alpha,\alpha',k,k',\sigma,\sigma'} J_{\alpha,\alpha'} \mathbf{S}^{\rm dot} \cdot \mathbf{S}^e_{\alpha'\alpha} \quad (1)$$

where $\mathbf{S}^{\rm dot} = f^\dagger_{\sigma'} \tau_{\sigma'\sigma} f_\sigma$, $\mathbf{S}^e_{\alpha\alpha'} = c^\dagger_{\alpha',k',\sigma'} \tau_{\sigma'\sigma} c_{\alpha,k,\sigma}$ are the spin-1/2 operators of the electron on the dot and in the leads, respectively, τ are Pauli matrices, and $\alpha,\alpha' = L/R, \sigma,\sigma' = \uparrow\downarrow$ are the lead and spin indices, respectively. $c^\dagger_{\alpha,k,\sigma}$ is the electron creation operator for the lead α with Fermi energies being $\mu_{L/R} = \pm V/2$, and f_σ is the pseudofermion operator. The conduction electron leads show the above-mentioned power-law (pseudogap) DOS with respect to their Fermi levels $\mu_{L/R}$. In the Kondo regime, the single-occupancy constraint of the pseudofermions is imposed: $\sum_\sigma f^\dagger_\sigma f_\sigma = 1$. Here, the dimensionless interlead and intralead Kondo couplings are denoted by $g_{LR} = N_0 J_{LR}$ and $g_{LL} = g_{RR} = N_0 J_{LL} = N_0 J_{RR}$, respectively, where $N_0 = \frac{1}{2D_0}$ and D_0 is the bandwidth cutoff of the leads. For simplicity, we consider here the symmetrical Kondo couplings: $g_{\alpha\beta} = g$.

In equilibrium, the one-loop RG scaling equation for g reads $\frac{\partial g}{\partial \ln D} = rg - 2g^2$.[14] The critical Kondo coupling $g_c = \frac{r}{2}$ separates the Kondo ($g > g_c$) from the unscreened local

moment (LM) phase ($g < g_c$). Much of the equilibrium critical properties can be obtained from the cutoff dependence of the renormalized Kondo coupling: $g^{\rm eq}(D) = \frac{g_c}{1+(D/T^*)^{-r}}$ with the crossover energy scale being $T^* = D_0(\frac{|g_c-g_0|}{g_0})^{\frac{1}{r}} \propto |g_c - g|^{\nu}$ and the correlation length exponent being $\nu = 1/r$.

At a finite bias voltage, however, the system is under steady-state nonequilibrium condition; the Fermi levels of the two leads are shifted by $\pm V/2$. Under various RG approaches, the Kondo interaction vertices under nonequilibrium condition in general depend not only on the cutoff scale D, but also on the electron energy (frequency).[20,21] We employ here a weak coupling one-loop frequency-dependent nonequilibrium RG approach of Refs. 9 and 20 which keeps track of energy of the incoming conduction electrons in the Kondo scattering.

To emphasize the generic features of nonequilibrium scaling near the QCP of our system, we focus here (without the loss of generality) on the p-h symmetric pseudogap Kondo model with $0 < r < r^* = 0.375$, where the QCP is stable against the p-h asymmetry.[12–14] Experimentally, it is feasible to realize a p-h symmetric Kondo dot by controlling gate voltages. Note, however, that our approach is in general valid for any $r < 1$, though it works better for r being small. For $r > r*$, this QCP is unstable toward a different QCP with p-h asymmetry,[14] which exceeds the scope of this paper and will be addressed elsewhere. The nonequilibrium scaling equation for the Kondo couplings of our model under the approaches in Refs. 20 and 22 reads

$$\frac{\partial g_{\alpha\alpha'}(\omega)}{\partial \ln D} = \sum_{\beta=L,R}\left[\frac{r}{2}g_{\alpha\alpha'}(\omega) - g_{\alpha\beta}(\omega)g_{\beta\alpha'}(\omega)\right] \times \tanh\left(\frac{D}{2T}\right)\Theta\left(D - \left|\omega + \frac{\beta V}{2} + i\Gamma\right|\right), \tag{2}$$

$$\Gamma = \pi \sum_{\alpha\alpha'=L,R}\int d\omega f^{\alpha}_{\omega}\left(1 - f^{\alpha'}_{\omega}\right)[g_{\alpha\alpha'}]^2(\omega), \tag{3}$$

where $\alpha,\alpha' = L,R$, Γ is the current-induced decoherence rate obtained from the imaginary part of the pseudofermion self-energy,[20] $f^{\alpha}_{\omega} = \frac{1}{e^{\frac{\omega-\mu_\alpha}{T}}+1}$ is the Fermi function of the α lead, and $k_B = \hbar = e = 1$. Note that in equilibrium at a finite temperature T the RG flows of the Kondo couplings are cut off by T. Note that within the nonequilibrium RG approach, however, there are two cutoff scales: The couplings involving transferring electrons from one lead to the other $[g_{LR}(\omega = V/2)]$ are cut off by the bias voltage V through $\Theta(D - V)$; while as the ones involving electrons on the same lead $[g_{\alpha\alpha}(\omega = V/2)]$ are cut off by the decoherence rate $\Gamma \ll V$, a much lower energy scale than V (Ref. 20) via $\Theta(D - \Gamma)$ [see Eq. (2)]. Hence, the RG flows are not completely stopped until a much lower energy scale $D \leqslant \Gamma \ll V$ is reached. We shall focus below on the distinct nonequilibrium quantum critical behaviors due to this peculiar nonequilibrium RG flow.

We have numerically and analytically solved Eqs. (2) and (3) self-consistently at $T = 0$ in the limit of $D \to 0$ for a symmetrically coupled single-channel Kondo dot with $g_{\alpha\beta}(\omega) = g_{\alpha\alpha}(\omega) = g(\omega)$.[20] Note that our results are robust against the parity (left-right) asymmetry.[20] As shown in Fig. 1, for $g > (<) g_c$, the renormalized Kondo couplings exhibit peaks (dips) at $\omega = \pm V/2$, indicating Kondo (local moment) phase; while $g(\omega)$ is completely flat at criticality $g = g_c$. The qualitative nature of these peaks (dips) in $g(\omega)$ agree well with Refs. 9 and 10 as signatures of conducting (insulating) behavior. The height (depth) of the peaks (dips) get shorter (shallower) as one reaches to QCP from the Kondo (LM) phase. Here, we focus on the LM phase ($g \leqslant g_c$) where the perturbative RG approach is controlled. The full analytical and numerical solutions for $g(\omega)$ in the LM phase in the limit of $D \to 0$ are found to be

$$\begin{aligned}
g(\omega) &= g_0 + g_1(\omega) + g_2(\omega),\\
g_1(\omega) &= \frac{g_0(1+\tilde{V}^r)\left(\left|\tilde{\omega} - \frac{\tilde{V}}{2}\right|^r - 1\right)}{2(1+\tilde{V}^r)\left(1 + \left|\tilde{\omega} - \frac{\tilde{V}}{2}\right|^r\right)}\Theta\left(\tilde{D}_0 - \left|\tilde{\omega} - \frac{\tilde{V}}{2}\right|\right)\\
&\quad + \frac{g_c\left(\tilde{V}^r - \left|\tilde{\omega} - \frac{\tilde{V}}{2}\right|^r\right)}{2(1+\tilde{V}^r)\left(1 + \left|\tilde{\omega} - \frac{\tilde{V}}{2}\right|^r\right)}\Theta\left(\tilde{V} - \left|\tilde{\omega} - \frac{\tilde{V}}{2}\right|\right)\\
&\quad + (\omega \to -\omega),\\
g_2(\omega) &= \left(\frac{g_c\tilde{V}^{\frac{r}{2}}}{1+\tilde{V}^r}\right)\left\{\frac{\tilde{V}^{\frac{r}{2}} - \left|\tilde{\omega} - \frac{\tilde{V}}{2}\right|^{\frac{r}{2}}}{1 + \tilde{V}^{\frac{r}{2}}\left|\tilde{\omega} - \frac{\tilde{V}}{2}\right|^{\frac{r}{2}}}\right.\\
&\quad \times\left[\Theta\left(\tilde{\Gamma} - \left|\tilde{\omega} - \frac{\tilde{V}}{2}\right|\right) - \Theta\left(\tilde{V} - \left|\tilde{\omega} - \frac{\tilde{V}}{2}\right|\right)\right]\\
&\quad \left. + \frac{\tilde{\Gamma}^{\frac{r}{2}} - \tilde{V}^{\frac{r}{2}}}{1 + (\tilde{V}\tilde{\Gamma})^{\frac{r}{2}}}\Theta\left(\tilde{\Gamma} - \left|\tilde{\omega} - \frac{\tilde{V}}{2}\right|\right)\right\}\\
&\quad + (\omega \to -\omega),
\end{aligned} \tag{4}$$

with $\tilde{V} = \frac{V}{T^*}$, $\tilde{\omega} = \frac{\omega}{T^*}$, $\tilde{D}_0 = \frac{D_0}{T^*}$, $\tilde{\Gamma} = \frac{\Gamma}{T^*}$, and g_0 being the bare Kondo coupling. As shown in Fig. 1, The peaks (dips) of $g(\omega)$ near $\omega = \pm V/2$ shows a power-law behavior: $|g(\omega) - g(\omega = \pm V/2)| \propto |\omega \mp \frac{V}{2}|^{\frac{r}{2}}$ with a width of Γ. We furthermore find analytically the universal scaling forms for $g(\omega = 0, V)$ and $g(\omega = \pm V/2, V)$. These properties will be used in the following analysis to determine various novel nonequilibrium scaling behaviors in the LM phase:

$$g(\omega = 0) = \frac{g_c}{1 + \left(\frac{V}{2T^*}\right)^{-r}}, \quad g\left(\omega = \frac{V}{2}\right) = \frac{g_c}{1 + \left(\frac{V\Gamma}{T^{*2}}\right)^{-\frac{r}{2}}}. \tag{5}$$

III. UNIVERSAL SCALING OF NONEQUILIBRIUM DECOHERENCE

The current-induced decoherence Γ which cuts off the RG flow is the key to understanding the nonequilibrium quantum criticality of our model, as all nonequilibrium observables depend crucially on the scaling behavior of Γ. As shown in Fig. 1 (inset), Γ/V in the LM phase exhibits perfect universal V/T^* scaling over a wide range $10^{-6} < V/T^* < 10^6$. The discovery of this generic universal scaling behavior for the nonequilibrium decoherence rate carries fundamental importance in the nonequilibroum quantum phase transition in Kondo systems. This also constitutes a surprising result since the highly nonlinear universal scaling of Γ/V in Kondo-related models was either absent in Refs. 9 and 10 or has not been reported.[6] We believe this slow crossover is related to the large correlation length exponent $\nu = 1/r$ of the model. To

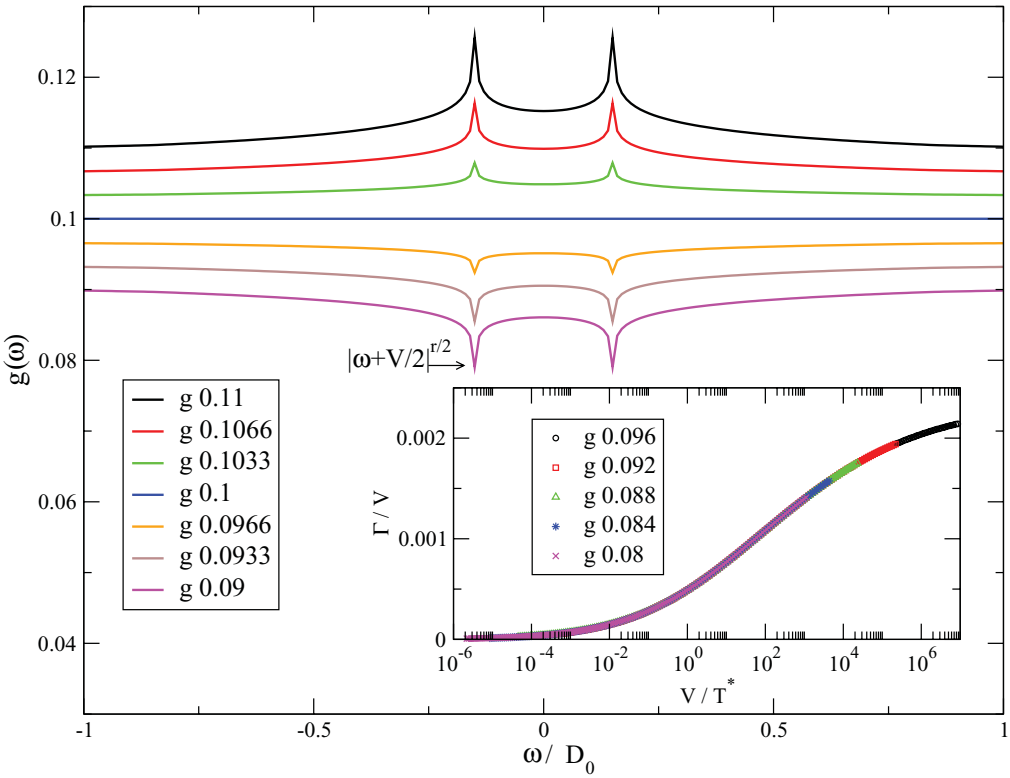

FIG. 1. (Color online) Renormalized Kondo coupling $g(\omega)$ for various bare couplings (in units of D_0) for $r = 0.2$ ($g_c = 0.1$). The bias voltage is $V = 0.3$. Inset: Universal scaling of Γ/V as a function of V/T^* with Γ being the decoherence rate.

gain more insight, we obtain the analytical approximated form $\Gamma/\pi \approx (1-\frac{\pi}{4})Vg^2(\omega=\frac{V}{2})+\frac{\pi}{4}Vg^2(\omega=0)$, where $g(\omega)$ is well approximated by a semiellipse for $-V/2<\omega<V/2$ [see the perfect agreement in Fig. 2(c) between dotted and dashed lines].[9] Via Eq. (5) the decoherence Γ at $T=0$ is approximated as

$$\frac{\Gamma}{\pi V} \approx \left(1-\frac{\pi}{4}\right)\frac{g_c^2}{\left[1+\left(\frac{V^2}{T^{*2}}\frac{\Gamma}{V}\right)^{-\frac{r}{2}}\right]^2}+\frac{\pi}{4}\frac{g_c^2}{\left[1+\left(\frac{V}{2T^*}\right)^{-r}\right]^2}. \tag{6}$$

It is clear from Eq. (6) that Γ/V is a universal scaling function of V/T^*. This well explains the scaling behavior obtained numerically (see Fig. 1 inset). We extract further the asymptotic power-law behaviors of Γ/V as a function of V/T^*. For $\Gamma \ll V \ll T^*$, we have $\frac{\Gamma}{\pi V} \approx \frac{\pi g_c^2}{4}(\frac{V}{2T^*})^{2r}$. For $V \gg \Gamma \gg T^*$, however, we find $\frac{\Gamma}{\pi V} \approx \frac{\pi g_c^2}{4}[1-2(\frac{V}{2T^*})^{-r}]$. At criticality, $\Gamma = \pi g_c^2 V$. The scaling behavior of the decoherence Γ [Fig. 2 and Eq. (6)], leading to distinct nonequilibrium scaling behaviors of all the observables discussed below, is our central result.

IV. CRITICAL PROPERTIES

A. The conduction electron T matrix

First, we analyze nonequilibrium critical properties on the conduction electron T matrix, defined by $G^R_{\alpha,\alpha',\sigma} = G^{R(0)}_{\alpha,\sigma}\delta_{\alpha,\alpha'} + G^{R(0)}_{\alpha,\sigma}T_{\alpha,\alpha',\sigma}(\omega)G^{R(0)}_{\alpha'\sigma}(\omega)$,[14,15] with $G^R_{\alpha,\alpha',\sigma}$, $G^{R(0)}_{\alpha,\alpha',\sigma}$ being the full and bare conduction electron Green's functions, respectively. The imaginary part of the T matrix $\mathrm{Im}[T(\omega)] \equiv T''(\omega)$ is directly proportional to the experimentally measurable tunneling density of states (TDOS) of our setup. Via renormalized perturbation theory up to second order [see Fig. 2(b) inset], we have

$$T^<_{\alpha\alpha'}(\omega) = \sum_{\beta=L,R}\int d\Omega\, g(\omega)g(\omega+\Omega) \times\left[\chi^R(\Omega)\tilde{G}^<_\beta + \chi^<(\Omega)\tilde{G}^A_\beta\right], \tag{7}$$

where $\chi(\Omega) = \int_{-\infty}^{\infty} dt\, e^{i\Omega t}\chi(t)$ with $\chi(t) \equiv -\langle T_c\{\mathbf{S}^{\mathrm{dot}}(t)\cdot\mathbf{S}^{\mathrm{dot}}(0)\}\rangle$ being the impurity susceptibility, $\tilde{G}^{<(A)}_\beta$ corresponds to the lesser (advanced) component of the conduction electron Green's functions with constant DOS [the effect of the pseudogap leads has been taken into account by the renormalized coupling $g(\omega)$], and $T^>_{\alpha\alpha'}(\omega) = T^<_{\alpha\alpha'}(-\omega)$. The imaginary part of the T matrix at $T=0$ is hence given by, at $T=0$,

$$-\pi T''_{\alpha\alpha'}(\omega) = \frac{3\pi^2}{8N(0)}g^2(\omega), \tag{8}$$

in agreement with the result in Ref. 23.

For $V=T=0$, $T''(\omega)_{\alpha\alpha'}$ in the LM phase exhibits a power-law dip near $\omega=0$, $T''(\omega)\propto|\omega|^{\frac{r}{2}}$. For $V>0$, this dip is split into two at $\omega=\pm\frac{V}{2}$ with the same power law: $T''(\omega)-T''(\omega=V/2)\propto|\omega-\frac{V}{2}|^{\frac{r}{2}}$. At the dips of $T''(\omega=\pm V/2)$, we find $T''(\omega=V/2)\propto g^2(\omega=V/2)$ shows a distinct nonequilibrium scaling behavior in V/T^* compared to that in equilibrium form $T''(\omega=0)\propto g^2(\omega=0)$. To extract this distinct scaling behavior more clearly, we define the

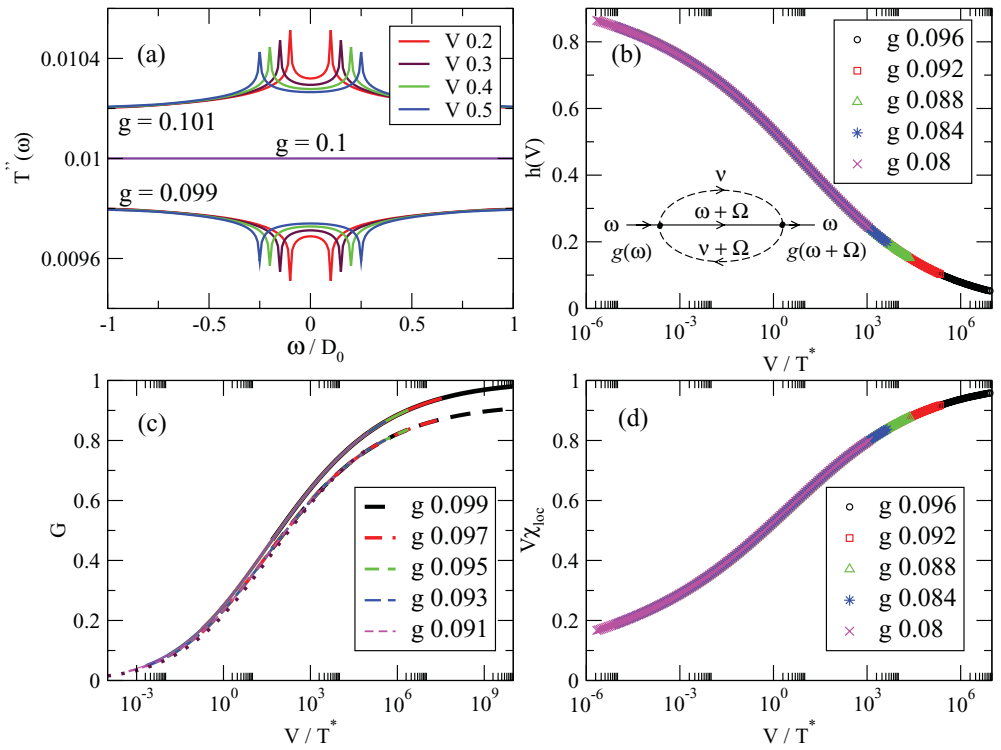

FIG. 2. (Color online) (a) The imaginary part of the T matrix $T''(\omega)$ (in units of $\frac{-3\pi}{8N(0)}$) versus V/T^* at $T=0$. (b) $h(V)$ defined in Eq. (9) versus V/T^*. Inset: the diagram for the T matrix. (c) The $T=0$ nonequilibrium conductance $G(V)$ (solid lines) normalized to $\frac{3\pi g_c^2}{4}$ in the LM phase versus V/T^* shows distinct scaling from the equilibrium counterpart, $G^{\rm eq}(T\to V)$ (dashed lines). The dotted line is the analytical form via Eq. (11). (d) The scaling of $V\chi_{\rm loc}$ versus V/T^*, with $\chi_{\rm loc}$ being the local impurity susceptibility. The bare Kondo couplings in (a)–(d) are in units of D_0, and $r=0.2$.

effective depth of the dips for $T''(\omega=\pm V/2)$, estimated as

$$h(V)\equiv\left|\frac{T''(\omega=V/2)-T''(\omega=0)}{T''(\omega=0)}\right| \approx\left|1-\frac{g^2(\omega=V/2)}{g^2(\omega=0)}\right|. \tag{9}$$

Hence, $h(V)$ in the LM phase follows a universal scaling function of V/T^* [see Fig. 2(b)] with the asymptotic behaviors $h(V)\approx 1-(\frac{4\Gamma}{V})^r$ for $\Gamma\ll V\ll T^*$; while for $T^*\ll\Gamma\ll V$, $h(V)\approx 2[(\frac{V\Gamma}{T^{*2}})^{-\frac{r}{2}}-(\frac{V}{2T^*})^{-r}]$. This new nonequilibrium scaling function $h(V)$ can be detected via the STM measurement on the leads.

B. The nonequilibrium conductance

Next, we turn our attention to transport properties. The nonequilibrium current I via the Fermi-Golden rule reads[9,20]

$$I=\frac{3\pi}{4}\int d\omega\left[\sum_\sigma g_{LR}(\omega)^2 f_\omega^L(1-f_\omega^R)\right]-(L\leftrightarrow R). \tag{10}$$

The current I is computed numerically by Eq. (10), and is approximated as[9] $I\approx\frac{3\pi}{4}[(1-\frac{\pi}{4})Vg^2(\omega=\frac{V}{2})+\frac{\pi}{4}Vg^2(\omega=0)]$. The differential conductance is readily obtained numerically via $G=\frac{\partial I}{\partial V}$. In the LM phase, it can be analytically approximated by

$$G(V)\approx\frac{3\pi g_c^2}{4}\left(1-\frac{\pi}{4}\right)\frac{\left[1+(1+r)\left(\frac{V\Gamma}{T^{*2}}\right)^{-\frac{r}{2}}\right]}{\left[1+\left(\frac{V\Gamma}{T^{*2}}\right)^{-\frac{r}{2}}\right]^3} +\frac{3\pi^2 g_c^2}{16}\frac{\left[1+(1+2r)\left(\frac{V}{2T^*}\right)^{-r}\right]}{\left[1+\left(\frac{V}{2T^*}\right)^{-r}\right]^3}. \tag{11}$$

As shown in Fig. 2(c), for $T^*\ll V\ll D_0$, $G(V)$ approaches the equilibrium scaling form

$$G^{\rm eq}(V\to T)\approx\frac{3\pi}{4}g^{\rm eq}(T)^2=\frac{\frac{3\pi}{4}g_c^2}{[1+(T/T^*)^{-r}]^2}, \tag{12}$$

while for $V/T^*\gg 1$ it exhibits a distinct universal scaling behavior of V/T^*. The perfect scaling behavior of $G(V/T^*)$ is a direct consequence of the perfect V/T^* scaling in Γ/V. By contrast, the universal V/T^* scaling for $G(V)$ is absent in Ref. 9 as Γ/V is not a universal function of V/T^* there. For $\Gamma\ll V\ll T^*$, the conductance behaves as $G(V)\approx[a(\frac{V}{2T^*})^{2r}+b(\frac{V}{T^*})^{2r+2r^2}]$ with $a=\frac{3\pi^2r^2}{64}$ and $b=\frac{3\pi r^2}{16}(1-\frac{\pi}{4})(\frac{r^2}{8})^r$, which shows a prefactor reduction with respect to its equilibrium form $G^{\rm eq}(V\to T\ll T^*)\approx\frac{3\pi r^2}{16}(\frac{T}{T^*})^{2r}$ and a subleading anomalous power law $\propto V^{2r+2r^2}$. For $V\gg\Gamma\gg T^*$, however, we find $G(V)\approx\frac{3\pi^2r^2}{64}[1-p(\frac{V}{2T^*})^{-r}-q(\frac{V}{T^*})^{-2r}]$ with $p=1-r$ and $q=\frac{8}{\pi}(1-\frac{\pi}{4})(1-r)(\frac{r^2}{8})^{-\frac{r}{2}}$, which

deviates significantly from its equilibrium form $G^{\rm eq}(V \to T \gg T^*) \approx \frac{3\pi r^2}{16}[1-2(\frac{T}{T^*})^{-r}]$. It is worthwhile emphasizing that, due to the very different role played by the bias V and temperature T, $G(V)$ follows a completely different scaling function from its equilibrium form $G^{\rm eq}(V \to T)$ over the full range of V/T^*, though it tends to converge with its equilibrium form for $V \ll T^*$.

C. Local spin susceptibility

Finally, we analyze the scaling behaviors of the local spin susceptibility $\chi_{\rm loc}(V) \equiv \frac{\partial M}{\partial h}|_{h\to 0}$ in the LM phase, with h being a small magnetic field and M being the magnetization $M = \frac{n_\uparrow - n_\downarrow}{n_\uparrow + n_\downarrow}$. The occupation number of the pseudofermion n_σ is obtained by solving the Keldysh component of the Dyson equation for the pseudofermion self-energy.[9,20] Following Refs. 9, 10, and 20 for $V \gg h \to 0$, we find [see Fig. 2(d)][24]

$$M \approx \frac{\int_{\frac{-V-h}{2}}^{\frac{-V+h}{2}} d\omega\, g^2(\omega)}{\int_{\frac{-V}{2}}^{\frac{V}{2}} d\omega\, g^2(\omega)}.$$

The approximated form for $V\chi_{\rm loc}$ reads [see Fig. 2(d)][24]

$$V\chi_{\rm loc} \approx \frac{g(\omega = V/2)^2}{\frac{\pi}{4} g(\omega=0)^2 + \left(1-\frac{\pi}{4}\right) g(\omega = V/2)^2}.$$

For $\Gamma \ll V \ll T^*$, $\chi_{\rm loc}$ exhibits an anomalous power-law behavior, $\chi_{\rm loc} \propto \frac{1}{V^{1-\eta_\chi}}$ with $\eta_\chi = 2r^2$, distinct from its equilibrium constant behavior $T\chi_{\rm loc}(T \ll T^*) \propto (g_c - g)^r$.[15] For $V \gg \Gamma \gg T^*$, however, we find $\chi_{\rm loc}$ acquires a power-law correction to the Curie behavior: $V\chi_{\rm loc} \approx 1 - V\Delta\chi_{\rm loc}$ and $\Delta\chi_{\rm loc} \propto \frac{1}{V^{1-\Delta\eta_\chi}}$ with an anomalous exponent $\Delta\eta_\chi = -r$; while its corresponding equilibrium form shows a different anomalous power-law behavior: $\chi_{\rm loc}(T \gg T^*) \propto \frac{1}{T^{1-\eta_\chi}}$ with $\eta_\chi = r^2$.[14,15] At criticality ($g = g_c$), $\chi_{\rm loc}$ shows perfect Curie law behavior: $\chi_{\rm loc} \propto 1/V$. These distinct nonequilibrium signatures near the QCP are detectable in local susceptibility measurements.

V. DISCUSSIONS AND CONCLUSIONS

Before we draw conclusions, we would like to make a few remarks here. First, our general approach and generic results open up the study of a fundamentally important new subject on the nonequilibrium quantum phase transitions in the PGK model. Meanwhile, though there has been no direct realization of the pseudogap fermionic leads with small $r < r^*$ reported so far, our results are relevant for describing the QPT out of equilibrium of a realistic Kondo quantum dot coupled to magnetic metal leads ($r = 0$), the so-called Bose-Fermi Kondo (BFK) model.[6–8] In this system, the spin fluctuations in the leads (magnons) act as vector bosons ($\mathbf{\Phi}$) coupled to the local spin on the dot via $H_{SB} = \gamma \mathbf{S}^{\rm dot} \cdot \mathbf{\Phi} + \sum_q \omega_q \mathbf{\Phi}_q^\dagger \cdot \mathbf{\Phi}_q$, where the bosonic bath exhibits sub-Ohmic spectral density: $\rho_b(\omega) \propto |\omega|^{1-\epsilon}$ with $\epsilon = \frac{1}{2}$. The equilibrium RG scaling equations read[7] $\frac{dg}{d\ln D} = \gamma^2 g - 2g^2$ and $\frac{d\gamma}{d\ln D} = \frac{\epsilon}{2}\gamma - \gamma^3$. One may study the effective Kondo model by fixing the spin-boson coupling at its critical value: $\gamma = \gamma_c = \sqrt{\epsilon/2}$. This leads to the change in the scaling dimension of the local spin operator to $[S^{\rm dot}] = \frac{\epsilon}{2}$,[7] and in that of the Kondo coupling g: $[g] = 1 + \frac{\epsilon}{2}$. The equilibrium RG scaling equation for the effective Kondo coupling of the BFK model (with $\gamma = \gamma_c$) hence reads $\frac{dg}{d\ln D} = \frac{\epsilon}{2} g - 2g^2$, which is equivalent to that for the PSG Kondo model with an effective pseudogap power-law exponent $\tilde{r} = \frac{\epsilon}{2} = \frac{1}{4} < r^*$.[25]

In conclusion, via a controlled frequency-dependent renormalization group approach we have investigated the quantum phase transition out of equilibrium in the pseudogap Kondo quantum dot. At zero temperature and finite bias voltage, we discovered in the local moment phase new quantum critical behaviors in the T matrix, conductance, and local spin susceptibility that are distinct from those in equilibrium and at finite temperatures. The key to explaining these differences is the nonequilibrium current-induced decoherence at a finite bias voltage, which acts quite differently from its equilibrium (zero bias but finite temperature) counterpart. This leads to distinct nonequilibrium behavior near the quantum phase transition. Our predictions offer a general and new perspective both theoretically and experimentally on the nonequilibrium quantum phase transitions in Kondo dots.

ACKNOWLEDGMENTS

We thank M. Vojta and S. Kirchner for many helpful discussions. This work is supported by the NSC Grant No. 98-2112-M-009-010-MY3, the MOE-ATU program, the CTS-NCTU, and the NCTS of Taiwan, R.O.C.

[1] S. Sachdev, *Quantum Phase Transitions* (Cambridge University Press, Cambridge, UK, 2000).
[2] R. M. Potok, I. G. Rau, H. Shtrikman, Y. Oreg, and D. Goldhaber-Gordon, Nature (London) **447**, 167 (2007).
[3] A. C. Hewson, *The Kondo Problem to Heavy Fermions* (Cambridge University Press, Cambridge, UK, 1997).
[4] A. G. Green and S. L. Sondhi, Phys. Rev. Lett. **95**, 267001 (2005).
[5] D. E. Feldman, Phys. Rev. Lett. **95**, 177201 (2005); A. Mitra, S. Takei, Y. B. Kim, and A. J. Millis, *ibid.* **97**, 236808 (2006).
[6] S. Kirchner and Q. M. Si, Phys. Rev. Lett. **103**, 206401 (2009).
[7] M. Kircan and M. Vojta, Phys. Rev. B **69**, 174421 (2004).
[8] S. Kirchner, L. Zhu, Q. Si, and D. Natelson, Proc. Natl. Acad. Sci. **102**, 18824 (2005).
[9] C.-H. Chung, K. Le Hur, M. Vojta, and P. Wölfle, Phys. Rev. Lett. **102**, 216803 (2009).
[10] C. H. Chung, K. V. P. Latha, K. Le Hur, M. Vojta, and P. Wölfle, Phys. Rev. B **82**, 115325 (2010).
[11] D. Withoff and E. Fradkin, Phys. Rev. Lett. **64**, 1835 (1990).
[12] C. Gonzalez-Buxton and K. Ingersent, Phys. Rev. B **57**, 14254 (1998).
[13] K. Ingersent and Q. Si, Phys. Rev. Lett. **89**, 076403 (2002).

[14]M. Vojta and L. Fritz, Phys. Rev. B **70**, 094502 (2004); L. Fritz and M. Vojta, *ibid*. **70**, 214427 (2004).
[15]L. Fritz, S. Florens, M. Vojta, Phys. Rev. B **74**, 144410 (2006).
[16]J. Hopkinson, K. Le Hur, E. Dupont, Physica B **359-361**, 1454 (2005).
[17]M. Vojta, L. Fritz, and R. Bulla, Europhys. Lett. **90**, 27006 (2010).
[18]L. G. G. V. Dias da Silva, N. Sandler, P. Simon, K. Ingersent, and S. E. Ulloa, Phys. Rev. Lett. **102**, 166806 (2009).
[19]The crossover scale T^* associated with the "true" QPT is a power-law function of the distance $t = |g - g_c|$ to QCP; it depends exponentially on t for QPTs of the KT type.
[20]A. Rosch, J. Paaske, J. Kroha, and P. Wölfle, Phys. Rev. Lett. **90**, 076804 (2003); J. Phys. Soc. Jpn. **74**, 118 (2005); J. Paaske, A. Rosch, and P. Wolfle, Phys. Rev. B **69**, 155330 (2004).
[21]S. Kehrein, Phys. Rev. Lett. **95**, 056602 (2005); S. G. Jakobs, V. Meden, and H. Schoeller, *ibid*. **99**, 150603 (2007).
[22]H. Schmidt and P. Wölfle, Ann. Phys. (Berlin) **19**, 60 (2010).
[23]A. Mitra and A. Rosch, Phys. Rev. Lett. **106**, 106402 (2011).
[24]C.-H. Chung and K. V. P. Latha, Phys. Rev. B **82**, 085120 (2010).
[25]Our results in the equilibrium limit agree with those in Ref. 7 for metallic leads. Different critical properties were predicted in Refs. 6 and 8 via the SU(N) large-N approach, different from the RG approaches applied here and in Ref. 7.